Iranian Government for funding one of us (AB) for the duration of his PhD studentship.

References

AHTEE, A., AHTEE, M., GLAZER, A. M. & HEWAT, A. W. (1976). *Acta Cryst.* B32, 3243–3446.
BROWN, I. D. (1981). *Structure and Bonding in Crystals*, Vol. 2, edited by M.O'KEEFE & A. NAVROTSKY, pp. 1–30. London: Academic Press.
BROWN, I. D. & ALTERMATT, D. (1985). *Acta Cryst.* B41, 244–247.
JAFFE, B., COOK, W. R. & JAFFE, H. (1971). *Piezoelectric Ceramics*. London: Academic Press.
JONA, F., SHIRANE, G., MAZZI, F. & PEPINSKY, R. (1957). *Phys. Rev.* 105, 849–856.
MEGAW, H. D. & DARLINGTON, C. N. W. (1975). *Acta Cryst.* A31, 161–173.
MICHEL, C., MOREAU, J. M. & JAMES, W. J. (1971). *Acta Cryst.* B27, 501–503.
SHANNON, R. D. (1976). *Acta Cryst.* A32, 751–767.
SHIRANE, G. & HOSHINO, S. (1954). *Acta Cryst.* 7, 203–210.
THOMAS, N. W. (1989). *Acta Cryst.* B45, 337–345.
THOMAS, N. W. (1991*a*). *Acta Cryst.* B47, 180–191.
THOMAS, N. W. (1991*b*). *Acta Cryst.* B47, 597–608.
THOMAS, N. W. (1992). Unpublished.
THOMAS, N. W. (1993). Unpublished.
WILLIAMS, D. E. (1971). *Acta Cryst.* A27, 452–455.

Acta Cryst. (1994). B50, 560–566

Structural Relations and Tetrahedral Ordering Pattern of Synthetic Orthorhombic $Cs_2CdSi_5O_{12}$ Leucite: A Combined Synchrotron X-ray Powder Diffraction and Multinuclear MAS NMR Study

BY A. M. T. BELL

SERC Laboratory, Daresbury, Warrington WA4 4AD, England

S. A. T. REDFERN* AND C. M. B. HENDERSON

Department of Geology, The University, Manchester M13 9PL, England

AND S. C. KOHN†

Department of Physics, University of Warwick, Coventry CV4 7AL, England

(*Received* 3 *December* 1993; *accepted* 28 *March* 1994)

Abstract

A previously unknown leucite-related structure has been determined for synthetic $Cs_2CdSi_5O_{12}$. NMR spectroscopy shows that there are five distinct tetrahedral sites (*T*-sites) occupied by Si and one *T*-site occupied by Cd in the framework structure, while analysis of the synchrotron X-ray powder diffraction pattern establishes that this material is orthorhombic, *Pbca* [$R_I = 13.1\%$, $R_{wp} = 16.1\%$, $R_{exp} = 13.1\%$; eight formula units per unit cell; unit-cell parameters $a = 13.6714\ (1)$, $b = 13.8240\ (1)$, $c = 13.8939\ (1)$ Å, $V = 2625.83\ (6)$ Å^3]. Tetrahedral cation ordering rates for Si and Cd are sufficiently high for both hydrothermally and dry-synthesized samples to be fully ordered. The symmetry relations between leucites with $P2_1/c$ and *Pbca* structures are discussed and it is shown that such materials are related by a displacive phase transition, in which the number of *T*-sites is reduced from 12 in $P2_1/c$ to 6 in *Pbca*. The ^{29}Si MAS NMR data are, at present, less useful than the X-ray results for providing absolute *T*—O distances and *T*—O—*T* bond angles.

Introduction

As part of a wider attempt to understand the controls and consequences of tetrahedral cation ordering in compounds with framework structures, we are currently studying a series of synthetic leucite analogues having the general formula $X^{I}_{2}Y^{II}Si_5O_{12}$ (X = K, Rb, Cs; Y = Mg, Zn, Cd). These are related to natural leucite ($KAlSi_2O_6$) and pollucite ($CsAlSi_2O_6$) by the coupled tetrahedral framework cation substitution $2Al = Y + Si$ (Torres-Martinez & West, 1989). Such compounds are generally more amenable to tetrahedral site (*T*-site) analysis than Al–Si analogues and can also display significantly enhanced *T*-site ordering kinetics compared with the $KAlSi_2O_6$-type compound. For example, dry synthesized $K_2MgSi_5O_{12}$ leucite is cubic *Ia3d* with a dis-

* Present address: Department of Earth Sciences, University of Cambridge, Downing Street, Cambridge CB2 3EQ, England.
† Present address: Department of Geology, The University, Bristol BS8 1RJ, England.

ordered *T*-site distribution, but the corresponding hydrothermally synthesized sample is monoclinic $P2_1/c$ with ten Si and two Mg on 12 fully ordered *T*-sites (Bell *et al.*, 1994). In contrast, hydrothermally annealed $Cs_2CuSi_5O_{12}$ is believed to be tetragonal $P4_12_12$ with a distinctly different fully ordered *T*-site distribution having six sites occupied by Si and one by Cu (Heinrich & Baerlocher, 1991).

In this paper we report a structure determination for a dry-synthesized leucite analogue of stoichiometric $Cs_2CdSi_5O_{12}$, in which the results of synchrotron powder X-ray diffraction and magic angle spinning (MAS) NMR studies are integrated.* The principal value of the MAS NMR data in these systems is to determine the number of tetrahedral sites and to distinguish those which have four Si as next-nearest neighbours (NNN) from those with mixed Si and Y^{2+} NNNs. Thus, in a multi-nuclear (^{29}Si, ^{113}Cd and ^{133}Cs) MAS NMR study of this material (Kohn, Henderson & Dupree, 1994), the ^{29}Si spectrum (Fig. 1) was found to consist of five peaks of approximately equal intensity, indicating the presence of five distinct Si sites. In addition, the Cd and Cs NMR spectra directly confirm the presence of one Cd site (making a total of six *T*-sites) and two different cavity cation sites containing Cs.

Experimental

Appropriate proportions of Cs_2CO_3, $CdCO_3$ and SiO_2 glass were ground together and heated to *ca* 873 K overnight to decompose the carbonates. This mixture was melted at 1423 K for 24 h and then quenched by dipping the bottom of the platinum crucible in water. Chemical and electron microprobe analyses show that the glass starting material is homogeneous and 'on composition' within analytical error (formula $Cs_{2.08}Cd_{1.02}Si_{4.97}O_{12}$). The finely ground glass was then crystallized at 1123 K and 1 atm. pressure for 5 days to produce the dry-synthesized sample.

The ^{29}Si MAS NMR spectrum was obtained using a Bruker MSL 360 spectrometer (8.45 T) operating at 71.5 MHz. In order to determine the exact crystal structure and *T*-site ordering pattern of this sample, an X-ray powder diffraction study on this material has been carried out using the high-resolution powder diffractometer on Station 2.3 of the SERC Daresbury Laboratory synchrotron radiation source (Cernik, Murray, Pattison & Fitch, 1990; Collins, Cernik, Pattison, Bell & Fitch, 1992). Analysis of the powder diffraction data shows that $Cs_2CdSi_5O_{12}$ has the orthorhombic space group *Pbca*, a previously unknown version of the leucite structure type. All the different leucite-related structures have the same tetrahedral framework topology, allowing the starting model for the refinement to be based on the atomic coordinates for cubic (*Ia3d*) $K_2MgSi_5O_{12}$ (Bell *et al.*, 1994) transferred to the orthorhombic *Pbca* cell. All the cubic coordinates could be related by the symmetry operations for *Pbca*. In the *Pbca* cell, the only Wyckoff position that could accommodate any of the atoms is the 8*c* general position. To accommodate 48 *T*-site atoms, six different 8*c* positions are required, which confirms the deduction of six *T*-sites (five Si and one Cd) based on the NMR results (Kohn, Henderson & Dupree, 1994).

The $Cs_2CdSi_5O_{12}$ structure was then refined by the Rietveld method (Rietveld, 1969) using *MPROF* in the Powder Diffraction Program Library (Murray, Cockcroft & Fitch, 1990). In the starting model, the Si and Cd atoms were initially assumed to be disordered over the six *T*-sites. The *T*—O distances were all constrained (Rollet, 1970; Pawley, 1972) to be 1.68 (2) Å, intermediate between Si—O and Cd—O tetrahedral bond lengths. As the refinement progressed, it soon became apparent that one *T*—O distance was significantly larger than the other five; this *T*-site atom was then assigned as Cd(1) and the other five as Si atoms. The *T*—O distances in the CdO_4 tetrahedral unit were constrained to be the same (±0.02 Å) and the *T*—O distances for the five SiO_4 units were constrained to be 1.61 (2) Å, a suitable average Si—O distance for tetrahedrally coordinated Si [*International Tables for X-ray Crystallography* (1974, Vol. III)] and the refinement continued almost to convergence.

The constraints on the SiO_4 units were then changed so that the *T*—O distances in each unit were constrained to be the same (±0.02 Å), but the mean distance for each tetrahedron was allowed to differ. The refinement then continued to complete convergence.

* A list of powder diffraction data has been deposited with the IUCr (Reference: LI0172). Copies may be obtained through The Managing Editor, International Union of Crystallography, 5 Abbey Square, Chester CH1 2HU, England.

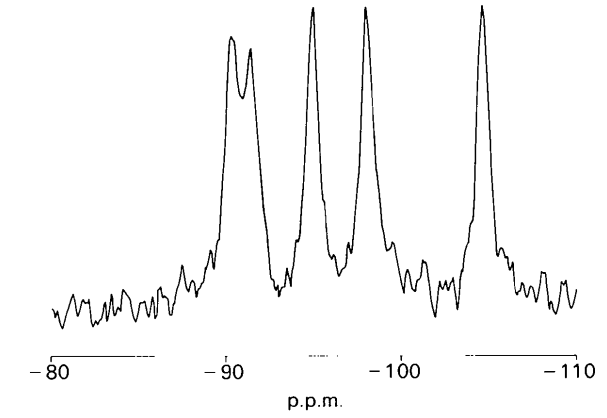

Fig. 1. ^{29}Si MAS NMR spectrum of $Cs_2CdSi_5O_{12}$ leucite.

Results

The observed and calculated profiles in the Rietveld difference plot show good agreement (Fig. 2), except that some of the strong *h*00 reflections show the effects of preferred orientation. The agreement indicates that the refined structure is reliable. The final refined structural parameters and *R* factors are given in Table 1 and the calculated bond lengths and angles in Tables 2–5.

The mean Si—O bond length is within the range observed for framework silicates, but note the very low value for the Si(4) tetrahedron (Table 2). The tetrahedral Cd—O bond length is close to the value (2.18 Å) obtained from the data of Shannon (1976). Mean Cs—O bond lengths (Table 5) are slightly larger than for the K—O polyhedra in the ordered form of $K_2MgSi_5O_{12}$ (3.20–3.42 Å; Bell *et al.*, 1994), but are about the same as for Cs—O in pollucite (3.39 and 3.56 Å; Beger, 1969).

As expected, the large CdO_4 tetrahedron has a significantly higher O—*T*—O angle variance (94.2 deg^2) than the mean variance for the SiO_4 tetrahedra (46.8 deg^2) (Table 3). Equivalent values for SiO_4 and MgO_4 in $K_2MgSi_5O_{12}$ are 20.9 and 40.4 deg^2 (Bell *et al.*, 1994), and for SiO_4 and CuO_4 in $Cs_2CuSi_5O_{12}$ are 22.7 and 140 deg^2 (Heinrich & Baerlocher, 1991). Thus, in all cases, the divalent cation tetrahedra are the more distorted, reflecting their greater 'flexibility' in the framework. As might be expected, the larger CdO_4 is more distorted than the smaller MgO_4, but the CuO_4 tetrahedron is the most distorted, perhaps due to Jahn–Teller effects.

The mean *T*—O—*T* angles (Table 4) show that the smallest angle (126.5°) is associated with the Cd—O tetrahedron, in agreement with the usual inverse relationship between mean *T*—O bond length and mean *T*—O—*T* angle shown by framework silicates (Hill & Gibbs, 1979).

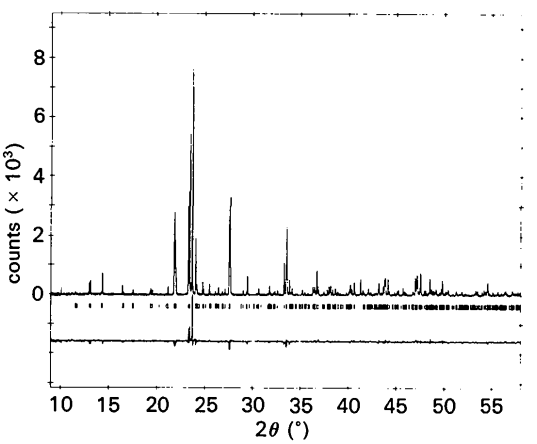

Fig. 2. Rietveld plot for $Cs_2CdSi_5O_{12}$ leucite, showing observed, calculated and difference patterns.

Table 1. *Refined structural parameters for* $Cs_2CdSi_5O_{12}$

		x	*y*	*z*	B_{iso}
Cs(1)	8(*c*)	0.1261 (3)	0.1302 (2)	0.1521 (2)	3.44 (6)
Cs(2)	8(*c*)	0.3743 (3)	0.3866 (2)	0.3841 (2)	3.44 (6)
Cd(1)	8(*c*)	0.3790 (3)	0.8372 (3)	0.9379 (2)	2.86 (9)
Si(2)	8(*c*)	0.124 (1)	0.6674 (8)	0.6002 (8)	0.7 (1)
Si(3)	8(*c*)	0.5868 (8)	0.1111 (9)	0.6342 (9)	0.7 (1)
Si(4)	8(*c*)	0.6424 (9)	0.6021 (8)	0.1064 (9)	0.7 (1)
Si(5)	8(*c*)	0.894 (1)	0.3701 (9)	0.8128 (8)	0.7 (1)
Si(6)	8(*c*)	0.8274 (9)	0.9177 (9)	0.343 (1)	0.7 (1)
O(1)	8(*c*)	0.470 (1)	0.370 (2)	0.152 (2)	0.2 (2)
O(2)	8(*c*)	0.102 (2)	0.498 (1)	0.406 (1)	0.2 (2)
O(3)	8(*c*)	0.375 (2)	0.168 (1)	0.483 (1)	0.2 (2)
O(4)	8(*c*)	0.749 (1)	0.427 (1)	0.608 (1)	0.2 (2)
O(5)	8(*c*)	0.642 (2)	0.717 (1)	0.380 (1)	0.2 (2)
O(6)	8(*c*)	0.368 (2)	0.623 (1)	0.762 (1)	0.2 (2)
O(7)	8(*c*)	0.998 (1)	0.886 (1)	0.659 (1)	0.2 (2)
O(8)	8(*c*)	0.661 (1)	0.962 (1)	0.849 (1)	0.2 (2)
O(9)	8(*c*)	0.909 (1)	0.643 (2)	0.905 (1)	0.2 (2)
O(10)	8(*c*)	0.207 (1)	0.896 (2)	0.140 (2)	0.2 (2)
O(11)	8(*c*)	0.131 (2)	0.174 (1)	0.949 (1)	0.2 (2)
O(12)	8(*c*)	0.886 (2)	0.150 (1)	0.200 (1)	0.2 (2)

R_I = 13.1%, R_{wp} = 16.1%, R_{exp} = 13.1%; *a* = 13.6714 (1), *b* = 13.8240 (1), *c* = 13.8939 (1) Å, *V* = 2625.83 (6) Å^3.

Table 2. *T*—O *bond lengths* (Å) *for* $Cs_2CdSi_5O_{12}$

Cd(1)—O(4)	2.24 (2)	Si(4)—O(2)	1.54 (2)
Cd(1)—O(7)	2.21 (2)	Si(4)—O(3)	1.55 (2)
Cd(1)—O(9)	2.24 (1)	Si(4)—O(4)	1.53 (2)
Cd(1)—O(11)	2.27 (1)	Si(4)—O(12)	1.51 (2)
Mean	2.24 (2)	Mean	1.53 (2)
Si(2)—O(1)	1.56 (2)	Si(5)—O(5)	1.60 (2)
Si(2)—O(3)	1.63 (2)	Si(5)—O(7)	1.55 (2)
Si(2)—O(5)	1.65 (2)	Si(5)—O(8)	1.56 (2)
Si(2)—O(10)	1.54 (2)	Si(5)—O(12)	1.60 (2)
Mean	1.60 (5)	Mean	1.58 (3)
Si(3)—O(1)	1.64 (2)	Si(6)—O(6)	1.66 (2)
Si(3)—O(2)	1.62 (2)	Si(6)—O(8)	1.67 (2)
Si(3)—O(6)	1.57 (2)	Si(6)—O(9)	1.64 (2)
Si(3)—O(11)	1.57 (2)	Si(6)—O(10)	1.69 (2)
Mean	1.60 (4)	Mean	1.67 (2)

Overall mean Si—O 1.59 (5) Å.

Table 3. O—*T*—O *bond angles* (°) *for* $Cs_2CdSi_5O_{12}$

O(4)—Cd(1)—O(7)	103.5 (6)	O(2)—Si(4)—O(3)	114 (1)
O(4)—Cd(1)—O(9)	110.4 (7)	O(2)—Si(4)—O(4)	96 (1)
O(4)—Cd(1)—O(11)	121.6 (7)	O(2)—Si(4)—O(12)	113 (1)
O(7)—Cd(1)—O(9)	114.8 (7)	O(3)—Si(4)—O(4)	108 (1)
O(7)—Cd(1)—O(11)	113.1 (8)	O(3)—Si(4)—O(12)	113 (1)
O(9)—Cd(1)—O(11)	93.8 (7)	O(4)—Si(4)—O(12)	111 (1)
Mean	109.5 [94.2]*	Mean	109:2 [46.3]
O(1)—Si(2)—O(3)	118 (1)	O(5)—Si(5)—O(7)	105 (1)
O(1)—Si(2)—O(5)	112 (1)	O(5)—Si(5)—O(8)	106 (1)
O(1)—Si(2)—O(10)	105 (1)	O(5)—Si(5)—O(12)	115 (1)
O(3)—Si(2)—O(5)	99 (1)	O(7)—Si(5)—O(8)	105 (1)
O(3)—Si(2)—O(10)	111 (1)	O(7)—Si(5)—O(12)	110 (1)
O(5)—Si(2)—O(10)	113 (1)	O(8)—Si(5)—O(12)	115 (1)
Mean	109.7 [44.7]	Mean	109.3 [22.7]
O(1)—Si(3)—O(2)	109 (1)	O(6)—Si(6)—O(8)	110 (1)
O(1)—Si(3)—O(6)	103 (1)	O(6)—Si(6)—O(9)	93.7 (9)
O(1)—Si(3)—O(11)	114 (1)	O(6)—Si(6)—O(10)	113 (1)
O(2)—Si(3)—O(6)	110 (1)	O(8)—Si(6)—O(9)	115 (1)
O(2)—Si(3)—O(11)	103 (1)	O(8)—Si(6)—O(10)	105 (1)
O(6)—Si(3)—O(11)	118 (1)	O(9)—Si(6)—O(10)	120 (1)
Mean	109.5 [35.5]	Mean	109.4 [84.6]

Mean variance for SiO_4 = 187.4 (46.8).

* Tetrahedral angle variance [σ^2, deg^2]: $\sigma^2 = \Sigma(\theta - 109.47)^2/5$ (Robinson, Gibbs & Ribbe, 1971).

Table 4. *T*—O—*T bond angles* (°) *for* $Cs_2CdSi_5O_{12}$

Si(2)—O(1)—Si(3)	142 (2)	Cd(1)—O(7)—Si(5)	144 (1)
Si(3)—O(2)—Si(4)	152 (2)	Cd(1)—O(9)—Si(6)	117 (1)
Si(2)—O(3)—Si(4)	143 (1)	Cd(1)—O(11)—Si(3)	118 (1)
Si(2)—O(5)—Si(5)	142 (1)	Mean Cd—O—Si	127 (13)
Si(3)—O(6)—Si(6)	154 (1)	Mean Si(2)—O—*T*	145 (4)
Si(5)—O(8)—Si(6)	147 (1)	Mean Si(3)—O—*T*	142 (16)
Si(2)—O(10)—Si(6)	151 (2)	Mean Si(4)—O—*T*	141 (10)
Si(4)—O(12)—Si(5)	142 (2)	Mean Si(5)—O—*T*	144 (2)
Mean Si—O—Si	147 (5)	Mean Si(6)—O—*T*	142 (17)
Cd(1)—O(4)—Si(4)	127 (1)	Mean Cd(1)—O—*T*	127 (12)

Table 5. Cs—O *bond lengths* (Å) *for* $Cs_2CdSi_5O_{12}$

Cs(1)—O(1)	3.83 (2)	Cs(2)—O(1)	3.49 (2)
Cs(1)—O(2)	3.69 (2)	Cs(2)—O(2)	4.04 (2)
Cs(1)—O(2)	3.90 (1)	Cs(2)—O(3)	3.32 (2)
Cs(1)—O(4)	3.82 (1)	Cs(2)—O(4)	3.08 (2)
Cs(1)—O(5)	3.42 (2)	Cs(2)—O(5)	3.58 (2)
Cs(1)—O(6)	3.74 (2)	Cs(2)—O(6)	3.72 (3)
Cs(1)—O(7)	3.14 (2)	Cs(2)—O(7)	3.61 (2)
Cs(1)—O(8)	3.18 (2)	Cs(2)—O(8)	3.89 (2)
Cs(1)—O(9)	3.27 (2)	Cs(2)—O(9)	3.01 (2)
Cs(1)—O(10)	3.42 (2)	Cs(2)—O(10)	3.57 (2)
Cs(1)—O(11)	2.88 (2)	Cs(2)—O(11)	3.55 (2)
Cs(1)—O(12)	3.36 (3)	Cs(2)—O(12)	3.47 (1)
Mean Cs(1)—O	3.5 (4)	Mean Cs(2)—O	3.5 (3)

The tetrahedron connectivities (Table 4) show that Si(2) is linked to four next-nearest neighbour (NNN) Si tetrahedra [Q^4(4Si) using NMR notation]. The other Si tetrahedra are all linked to three SiO_4 and one CdO_4 NNN tetrahedral species [*i.e.*, Q^4(3Si,1Cd)]. Projections of the structure (Fig. 3) show that the tetrahedron connectivities form linked four- and six-rings. Note that four-rings containing only Q^4(3Si,1Cd) SiO_4 tetrahedra (medium-shaded) are aligned approximately in the (100) plane [Fig. 3(*a*)], while the four-rings approximately parallel to the (010) and (001) planes contain one CdO_4 tetrahedron (dark-shaded) and one Q^4(4Si) SiO_4 tetrahedron (light-shaded) opposite each other [Figs. 3(*b*) and (*c*)]. Since the CdO_4 tetrahedra are much larger than the SiO_4 tetrahedra, these latter four rings are significantly distorted compared with the more regular 'square' arrangements of those without Cd.

The ^{29}Si NMR chemical shift for the Q^4(4Si) tetrahedron is −104.7 p.p.m. (relative to tetramethylsilane) (Fig. 1 and Kohn, Henderson & Dupree, 1994) and is associated with a mean *T*—O—*T* angle of 144.5°. These values are similar to those of −104.5 p.p.m. and 146.8° for one of the Q^4(4Si) tetrahedra in the ordered form of $K_2MgSi_5O_{12}$. ^{29}Si chemical shifts for $Cs_2CdSi_5O_{12}$ can be predicted from the structural data presented in this paper using the equations of Dupree, Kohn, Henderson & Bell (1992), which relate the chemical shift and the mean *T*—O—*T* angle for each site. The equations predict shifts of −107.9 [Q^4(4Si)], −91.2, −91.3, −93.8 and −96.5 p.p.m. [Q^4(3Si,1Cd)], compared with the experimental values of −104.7, −90.5, −95.1, −95.1 and −98.1 p.p.m., respectively. Thus, the mean difference between the observed and predicted shifts (assuming that the assigned order for the shifts is correct) is 1.4 p.p.m., with the largest difference being 3.2 p.p.m. The calculation of the mean *T*—O—*T* angles from the chemical shifts is less successful. For the Q^4(4Si) peak, the prediction is 140.8° compared with the X-ray result of 144.5°. For the Q^4(3Si,1Cd) silicons, the predictions are 134.2, 135.4, 141.0 and 147.2°, *i.e.* a range of mean *T*—O—*T* angles for the Q^4(3Si,1Cd) sites of 13° compared with the X-ray result of 2.3°. The very poor quality of predictions of mean *T*—O—*T* angles is probably largely due to the wide variation of the individual *T*—O—*T* angles within a given tetrahe-

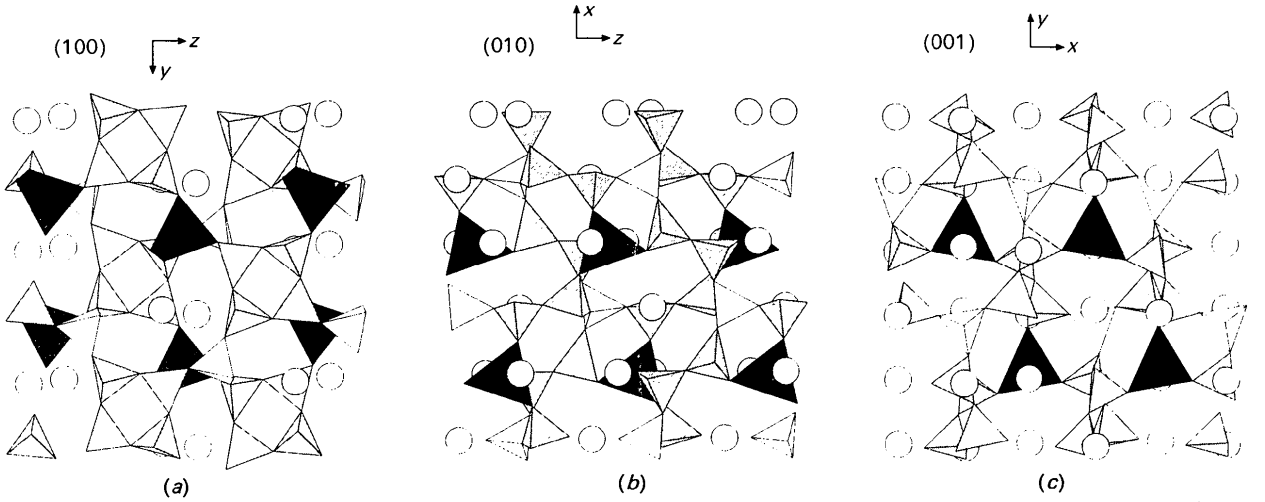

Fig. 3. Projected structure of $Cs_2CdSi_5O_{12}$ leucite: (*a*) on (100); (*b*) on (010); (*c*) on (001). Light-shaded tetrahedra are Q^4(4Si), medium-shaded are Q^4(3Si,1Cd) and dark-shaded are CdO_4 tetrahedra.

dron. For example, Si(5) has angles from 142 to 147°, whereas Si(6) has angles from 117 to 154°.

Discussion

Kohn, Dupree, Mortuza & Henderson (1991) and Bell *et al.* (1994) showed that the ordered form of $K_2MgSi_5O_{12}$ leucite has Si Q^4(4Si) and Mg tetrahedra, separated by one Si Q^4(3Si,1Mg) tetrahedron, occupying opposite corners of four rings, and in addition that a given tetrahedral species is separated by two tetrahedra from another of the same species. The $Cs_2CdSi_5O_{12}$ leucite exhibits exactly these types of connectivities (Fig. 3). The ordered K—Mg leucite, with 10 Si *T*-sites, has two Q^4(4Si) Si tetrahedra with different NNN tetrahedra and two types of Q^4(3Si,1Mg) SiO_4 units, two pairs with the same NNN tetrahedral species and four with different NNN species. In contrast, the $Cs_2CdSi_5O_{12}$ leucite has one Q^4(4Si) Si tetrahedron and two pairs of Q^4(3Si,1Cd) SiO_4 units with the same NNN tetrahedral species (Table 6).

The ordering arrangement of Cd(1) in $Cs_2CdSi_5O_{12}$ may be compared with that of Mg in $K_2MgSi_5O_{12}$ using the stylized structure diagrams shown in Fig. 4. In order to make such a compari-

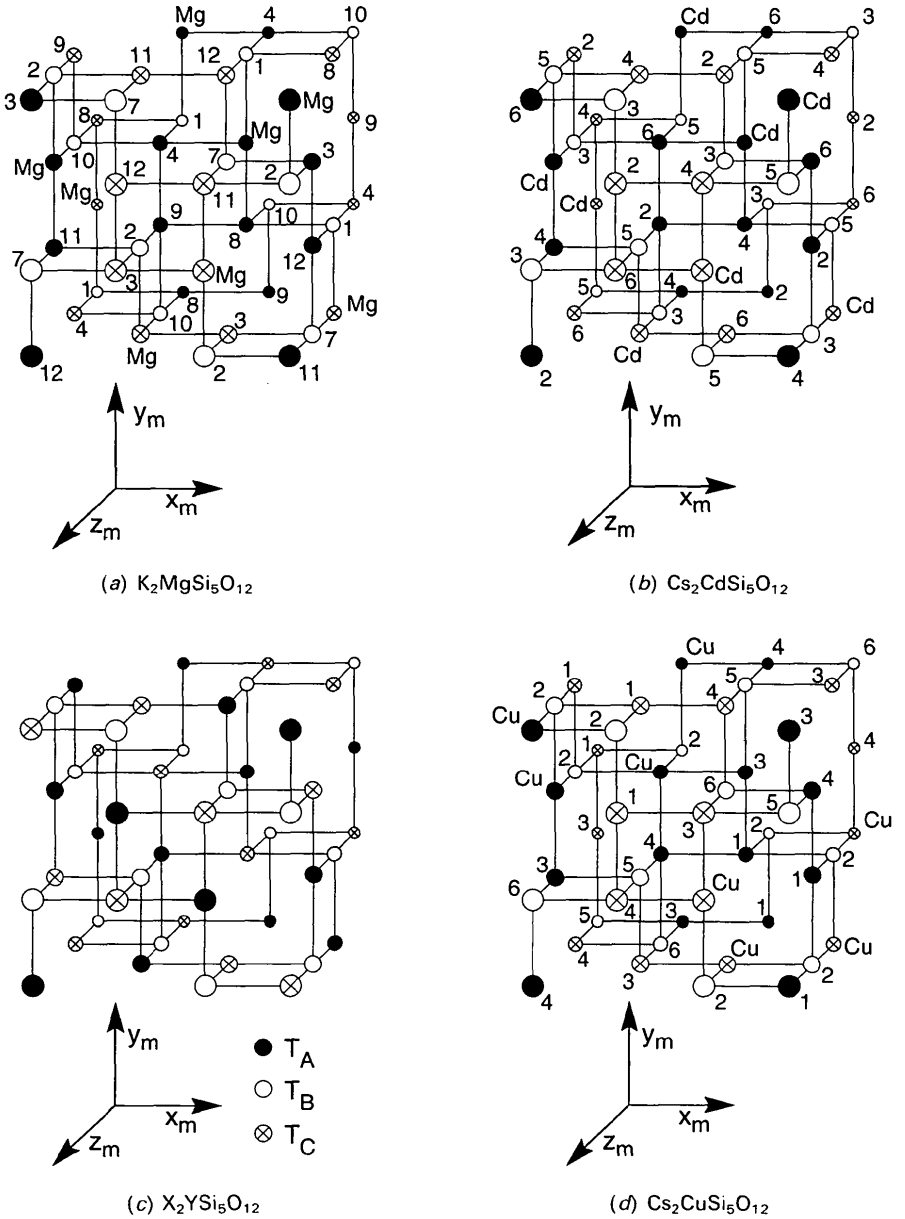

(*a*) $K_2MgSi_5O_{12}$ (*b*) $Cs_2CdSi_5O_{12}$

(*c*) $X_2YSi_5O_{12}$ (*d*) $Cs_2CuSi_5O_{12}$

Fig. 4. Schematic, idealized unit cells of several leucites (after Bell *et al.*, 1994): (*a*) hydrothermal $K_2MgSi_5O_{12}$ leucite (Bell *et al.*, 1994); (*b*) $Cs_2CdSi_5O_{12}$ leucite (this paper); (*c*) hypothetical disordered $Cs_2CdSi_5O_{12}$ leucite (this paper); (*d*) $Cs_2CuSi_5O_{12}$ leucite (Heinrich & Baerlocher, 1991). In (*a*), (*b*) and (*d*) the numbers refer to the Si-site species and the filled, open and crossed circles represent T_1, T_2 and T_3 sites in natural $I4_1/a$ leucite (Mazzi, Galli & Gottardi, 1976). The axes shown correspond to the coordinate system used by Mazzi, Galli & Gottardi (1976).

Table 6. *Connectivities of tetrahedra in* $Cs_2CdSi_5O_{12}$

T-site	Connected to			
Cd(1)	Si(3)	Si(4)	Si(5)	Si(6)
Si(2)	Si(3)	Si(4)	Si(5)	Si(6)
Si(3)	Cd(1)	Si(2)	Si(4)	Si(6)
Si(5)	Cd(1)	Si(2)	Si(4)	Si(6)
Si(4)	Cd(1)	Si(2)	Si(3)	Si(5)
Si(6)	Cd(1)	Si(2)	Si(3)	Si(5)

son, the orthorhombic cell has been transformed to the cell adopted by Mazzi, Galli & Gottardi (1976), according to $-z_{orth} \rightarrow x_m$, $-x_{orth} \rightarrow y_m$, $y_{orth}^{-1/2} \rightarrow z_m$ (where subscript m refers to the Mazzi coordinate system). Bell *et al.* (1994) made an analogous transformation of the coordinate system of $P2_1/c$ leucite in order to arrive at a similar graphical representation of the monoclinic structure. Direct comparison of the two structures shows that the 12 *T*-sites of monoclinic ($P2_1/c$) $K_2MgSi_5O_{12}$ are derived from the six *T*-sites of orthorhombic (*Pbca*) $Cs_2CdSi_5O_{12}$ leucite. Since $P2_1/c$ is a maximal subgroup of *Pbca* and the two unit cells are essentially the same size, this result is not unexpected; the correlation is clear in Figs. 4(*a*) and (*b*).

Examination of the connectivities of the six *T*-sites in the *Pbca* structure (Table 6) shows that Si(2) and Cd(1), Si(3) and Si(5), and Si(4) and Si(6) form three pairs of *T*-sites with similar connectivities. This suggests that the six *T*-sites in the orthorhombic structure could be reduced further to three *T*-sites (denoted T_A, T_B and T_C) by disordering the six tetrahedrally coordinated cations (five Si and one Cd) over these three sites. Note that Fig. 4(*c*) shows that these three *T*-sites have distinctly different NNN arrangements to those of the T_1, T_2 and T_3 sites observed in natural tetragonal leucite ($KAlSi_2O_6$), *i.e.* it is clear in Fig. 4(*c*) that no *T*-site is connected to other sites of the same type. In addition, the four rings parallel to $(001)_m$ do not show fourfold symmetry parallel to $[001]_m$ [Fig. 4(*c*)]. Rather, this disordered phase represents a possible orthorhombic leucite *T*-site ordering scheme with space group symmetry *Ibca*. Ultimately, the structure is derived from a cubic leucite with space group symmetry $Ia\bar{3}$ (Fig. 5). While the transition from *Pbca* to $P2_1/c$ symmetry may be accomplished by small movements of atoms (*i.e. via* a displacive phase transition), an *Ibca* structure could only be achieved in a compound of $X_2YSi_5O_{12}$ stoichiometry by disordering *Y* and Si over the *T*-sites. Therefore, the three *T*-site structure could only be expected to arise in these leucites by an order–disorder phase transition. $Cs_2CuSi_5O_{12}$ has been refined in the tetragonal $P4_12_12$ space group (Heinrich & Baerlocher, 1991) and apparently shows a completely different connectivity arrangement [Fig. 4(*d*)].

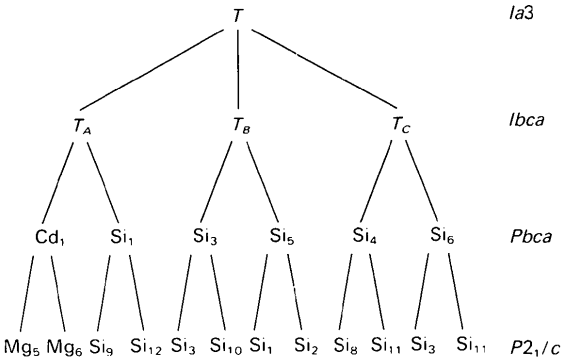

Fig. 5. *T*-site relationships for different leucite space groups. Note that the phase transitions between monoclinic $P2_1/c$ and orthorhombic *Pbca* and between orthorhombic *Ibca* and cubic $Ia\bar{3}$ are displacive, but that between *Pbca* and *Ibca* involves tetrahedral cation order–disorder.

The $Cs_2CdSi_5O_{12}$ leucite structure determined here differs from other leucites with similar stoichiometry such as $K_2MgSi_5O_{12}$, in that the Cd-substituted tetrahedra are very much larger than the Si-tetrahedra. Furthermore, unlike $K_2MgSi_5O_{12}$, the dry-synthesized $Cs_2CdSi_5O_{12}$ compound shows good long-range order and in this respect appears to be identical to hydrothermally synthesized samples, as indicated by the NMR results (Kohn, Henderson & Dupree, 1994). The *T*-site ordering kinetics in $Cs_2CdSi_5O_{12}$ are clearly greatly enhanced compared with the other leucite-type compounds studied so far. It seems likely that the larger size difference between Cd^{2+} and Si^{4+}, combined with the valency difference, control the ease with which this structure attains a high degree of long-range order.

The existence of an ordered orthorhombic leucite polymorph may have implications for our understanding of the high-temperature polymorphic behaviour of natural $KAlSi_2O_6$ leucite. On the transformation from low-temperature $I4_1/a$ leucite to the metrically cubic structure, an intermediate phase ($I4_1/acd$) is encountered over a limited temperature interval (Lange, Carmichael & Stebbins, 1986; Boysen, 1990). Group theoretical considerations (Palmer, 1990) show that an incommensurate (i.c.) structure might be locally stable over a limited temperature range between the tetragonal and cubic stability fields, but that such a structure would necessitate mixing of orthorhombic and tetragonal representations. Whether or not the orthorhombic *Ibca* symmetry described here could fulfil the requirements of the expected high-temperature orthorhombic component of the i.c. modulated phase remains to be established, but further investigations into the temperature-dependence of *T*-site ordering in these compounds should help to elucidate the more general sub-solidus behaviour of the leucite structure and are currently underway.

We thank the SERC for synchrotron beamtime and for access to the Chemical Database Service at the Daresbury Laboratory. The NMR work was supported by a research grant (GR3/7496) from NERC.

References

BEGER, R. M. (1969). *Z. Krist.* **129**, 280–302.
BELL, A. M. T., HENDERSON, C. M. B., REDFERN, S. A. T., CERNICK, R. J., CHAMPNESS, P. E., FITCH, A. N. & KOHN, S. C. (1994). *Acta Cryst.* B**50**, 31–41.
BOYSEN, H. (1990). Phase transitions in ferroelastic and coelastic crystals. In *Cambridge Topics in Mineral Physics and Chemistry*, edited by E. K. H. SALJE, pp. 334–349. Cambridge: Cambridge University Press.
CERNIK, R. J., MURRAY, P. K., PATTISON, P. & FITCH, A. N. (1990). *J. Appl. Cryst.* **23**, 292–296.
COLLINS, S. P., CERNIK, R. J., PATTISON, P., BELL, A. M. T. & FITCH, A. N. (1992). *Rev. Sci. Instrum.* **63**(1), 1013–1014.
DUPREE, R., KOHN, S. C., HENDERSON, C. M. B. & BELL, A. M. T. (1992). Calculation of NMR shielding constants and their use in the determination of the geometric and electronic structures of molecules and solids, edited by J. A. TOSSELL, NATO A.S.I. Vol., pp. 421–430.
HEINRICH, A. R. & BAERLOCHER, CH. (1991). *Acta Cryst.* C**47**, 237–241.
HILL, R. J. & GIBBS, G. V. (1979). *Acta Cryst.* B**35**, 25–30.
KOHN, S. C., DUPREE, R., MORTUZA, M. G. & HENDERSON, C. M. B. (1991). *Phys. Chem. Miner.* **18**, 144–152.
KOHN, S. C., HENDERSON, C. M. B. & DUPREE, R. (1994). *Phys. Chem. Miner.*, **21**. In the press.
LANGE, R. A., CARMICHAEL, I. S. E. & STEBBINS, J. F. (1986). *Am. Mineral.* **71**, 937–945.
MAZZI, F., GALLI, E. & GOTTARDI, G. (1976). *Am. Mineral.* **61**, 108–115.
MURRAY, A. D., COCKCROFT, J. K. & FITCH, A. N. (1990). Powder Diffraction Program Library (PDPL). Univ. College, London.
PALMER, D. C. (1990). Phase transitions in leucite. PhD Thesis, Cambridge Univ.
PAWLEY, G. S. (1972). *Advances in Structure Research by Diffraction Methods*, edited by W. HOPPE & R. MASON, Vol. 4, pp. 1–64. Oxford: Pergamon Press.
RIETVELD, H. M. (1969). *J. Appl. Cryst.* **2**, 65–71.
ROBINSON, K., GIBBS, G. V. & RIBBE, P. H. (1971). *Science*, **172**, 567–570.
ROLLET, J. S. (1970). *Crystallographic Computing*, edited by F. R. AHMED, p. 170. Copenhagen: Munksgaard.
SHANNON, R. D. (1976). *Acta Cryst.* A**32**, 751–767.
TORRES-MARTINEZ, L. M. & WEST, A. R. (1989). *Z. Anorg. Allg. Chem.* **573**, 223–230.

Acta Cryst. (1994). B**50**, 566–578

High-Resolution Neutron Study of Vitamin B_{12} Coenzyme at 15 K: Solvent Structure

BY J. P. BOUQUIERE

Crystallography Department, Birkbeck College, Malet Street, London WC1E 7HX, England

J. L. FINNEY

Department of Physics and Astronomy, University College London, Gower Street, London WC1E 6BT, England

AND H. F. J. SAVAGE

Chemistry Department, York University, Heslington YO1 5DD, England

(*Received* 27 *October* 1993; *accepted* 22 *February* 1994)

This paper is dedicated to the memory of the recent loss of Dr E. Lester Smith, a pioneer in the isolation of vitamin B_{12}

Abstract

The solvent structure of crystalline vitamin B_{12} coenzyme, determined from a high-resolution (0.9 Å) neutron data set collected at 15 K, is presented. The study involved the identification of solvent peaks and the formulation of possible solvent networks. The solvent distribution within the crystal can be described in two regions, namely (*a*) a channel, comprizing statically disordered water molecules and (*b*) leading into this channel, a region of highly ordered water molecules. The identification of the disordered solvent peaks has enabled the formulation of two main solvent networks per asymmetric unit, with the assistance of criteria used in the analyses of solvent structures in crystal hydrates of small molecules. The two networks comprise 17 water molecules each. A comparison of these solvent networks is made with those identified in a previous study of a crystal of the coenzyme at 279 K. The covalent and hydrogen-bond geometries involving the water molecules of these networks have been analysed and agree well with those found in small molecular crystal hydrates. Furthermore, the analysis of the water structure around apolar groups of the B_{12} coenzyme indicates the presence of clathrate-like water structures, as well as short distances which others have identified as C—H···O hydrogen bonds. Short range O···O non-hydrogen-bonded contacts obey known repulsive